# Thermo-Mechanical Analysis and Its Effect on Rf Behaviour of A Tapered Cavity of the W-Band Gyrotron Oscillator

**Sivavenkateswara Rao V, Muthiah Thottappan, Pradip Kumar Jain**

***Abstract*: Thermo-mechanical analysis of a tapered cylindrical RF interaction cavity of a $TE_{6,2}$, 95 GHz, 100 kW gyrotron has been carried out to study the effect of ohmic loss generated due to radiated microwave energy. For stable device operation, with the help of design relationships, describing the approach, an optimum thermal system design has been presented and performances got analyzed using a commercial simulation code "COMSOL Multiphysics". For various cavity thicknesses, and convective heat transfer coefficient values under without fins and with radial fins conditions system performance have been investigated. Taking water as coolant at ~293 K, hydraulic diameter and flow rate range has been determined for the optimum convective heat transfer coefficient values. An optimized simple cooling system thus designed keeps the maximum RF cavity radius deformation (increase) ~ 3.2 µm maintaining the average cavity outer surface temperature of 308 K. Further, using nonlinear time-dependent multimode analysis, a decrease of 48 MHz in resonance and a decrement of 20 in diffractive quality factor of the interaction cavity along with reduction of 2 kW of the device output power have been observed in the case for the deformed cavity from those of the initial cavity gyrotron device, which are found within the tolerance limit of such devices.***

***Index Terms*: Gyrotron Oscillator, Millimeter wave oscillator, RF cylindrical Cavity, Thermo-mechanical analysis.**

## I. INTRODUCTION

Gyrotron oscillator is a fast-wave electron-beam device capable of radiating long pulse/CW power of the order of hundred kWs to MWs in the millimeter and sub-millimeter wave regime and it operates on the principle of CRM instability. Gyrotrons are extensively used in various systems for the applications, like, material processing, electron cyclotron resonance heating (ECRH), electron cyclotron current drive (ECCD) and heat wave propagation experiments, etc. [1]-[3].Gyrotron consists of a magnetron injection gun (MIG) assembly that produces an annular gyrating electron beam, an RF interaction cavity surrounded by a superconducting magnet where the electron beam and RF wave interaction takes place, an RF extraction region to pass the RF power generated and a collector structure to gather the spent electron beam. The electron-beam and RF-wave interaction mechanism in gyrotron has been extensively investigated through theories as well as experiments by several groups [1]-[5]. However, limited studies reported for its thermo-mechanical management. A cylindrical tapered cavity is often used in the gyrotrons as its RF interaction structure, typically shown in Fig.1. It consists of three sections, viz., the input down-taper, middle uniform cylindrical section followed by up-taper section at the output side. The role of down taper is to prevent backward propagation of RF waves thereby protection of the emitter section of the device. Middle section is uniform cylindrical waveguide, is the region where the electron-beam and RF-wave interaction takes place and results in growth of the RF signal. The up-taper section converts standing-waves towards the end of the middle section into the travelling wave and thereby helps in propagating out the RF energy from the RF interaction cavity to the output section of the device. In gyrotron, apart from beam parameters, the RF structure dimension and its material properties also plays crucial role in the RF behavior of the device. Any changes in structural dimension and its material property of the RF interaction cavity not only causes deviation in its oscillation frequency but also degrades the RF output power as well as efficiency of the device apart from additional heating of the device structure. In the beam-wave interaction process, due to the finite electrical conductivity of the cavity walls, some part of the RF waves gets dissipated as the Ohmic loss [1], [3]. This leads to structure heating which may results in the RF cavity deformations,

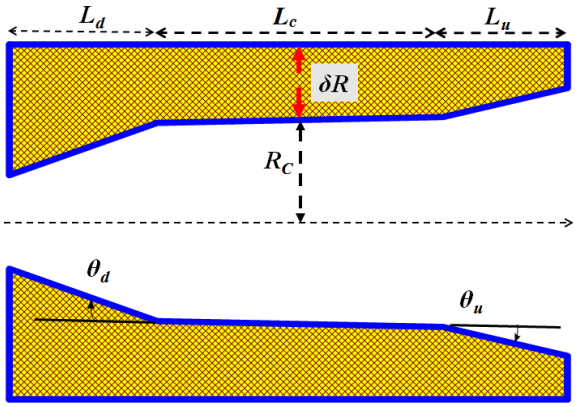


**Fig.1:** Schematic of a typical tapered cylindrical RF interaction cavity structure of the gyrotron ( $L_d$= down-taper length $L_c$=middle section length, $L_u$=up-taper length, $R_c$=cavity radius, $\delta R$=thickness of cavity from middle section $\theta_d$= down taper angle, and $\theta_u$=up-taper angle).

**Revised Manuscript Received on July 01, 2019.**

**Sivavenkateswara Rao V**, Department of Electronics Engineering, IIT (BHU) Varanasi, Varanasi, India.
**Muthiah Thottappan**, Department of Electronics Engineering, IIT (BHU) Varanasi, Varanasi, India.
**Pradip Kumar Jain**, Department of Electronics Engineering, National Institute of Technology Patna, Patna, India.

thereby changes in the oscillation frequency as well as decrease in the RF power output. Hence, an efficient thermal management system needs to be designed and ensured for stable operation of the gyrotron device [1], [3], [5]. Thermo-mechanical studies and its effect on RF behaviour of 1 MW power gyrotrons at 140 GHz, 170 GHz and 240 GHz has been investigated using computational fluid domain softwares, like, ANSYS, STAR CCM and COMSOL Multi-physics in [6]-[9]. J Koner and A K Sinha [9] have carried out thermal analysis of RF interaction cavity of a 200kW CW, 42GHz gyrotron using ANSYS code for different coolant flow rate with the axial fins provided on its outer surface. A Kumar et al. [6] extended this work for 170 GHz gyrotron with axial as well as radial cooling fins. Q Liu et al. [7], [8] also carried out heat transfer analysis of the RF interaction cavity for the 140 GHz and 240 GHz gyrotrons using ANSYS code and shown the effect of cavity deformations on the multi-mode beam-wave interaction of the device. However, cooling fins and thermal system design and its optimization for the RF cavity of the device is not reported. In the present work, the thermal and structural analysis of a tapered cylindrical RF interaction cavity of the gyrotron is carried out. With the help of design relationships, radial cooling fins design on the outer jacket of the middle section of the RF interaction cavity is presented. An optimum thermal system is designed and simulated using "COMSOL Multiphysics" code. Implementation of commercial code "COMSOL Multiphysics" is simpler than those used in previously reported work though equally accurate for this purpose and not explored earlier [10]. For the designed cooling system with different convective heat transfer coefficients, deformations in cavity profile are obtained through this simulation. Nonlinear time-dependent multimode theory is used further to obtain the RF output behavior of the gyrotrons [3], [11]-[13]. An optimum thermal system design thus obtained with maximum possible deformation in the inner dimension of the RF cavity ensures the gyrotron oscillator RF frequency and power output variations within the specified tolerance limit of the device.

The work is organized as follows. In Section II, the effects of the RF cavity deformations on the resonant frequency of the device, the ohmic loss analysis of tapered interaction cavity that acts as wall load, radial cooling fins design, role of cooling fins in the heat transfer enhancement and the heat transfer mechanisms of RF structure are presented. The thermo-mechanical analysis simulation set-up without fins and with radial fins using commercial code COMSOL Multiphysics is explained in Section III. In Section IV, the simulated results of the RF structure for various convective heat transfer coefficients for different fin groups under optimized values of thermal system parameters are presented followed by its effects on the RF performance of the device due to changed scenario of the electron beam and RF wave interaction are also presented. Finally, conclusions are drawn in Section V.

## II. ANALYSIS

In the present work, we have typically considered a tapered cylindrical RF interaction cavity for a 95 GHz, 100 kW gyrotron operating in $TE_{6,2}$ mode with beam voltage and current of 50 kV and 5 A, respectively, along with a background DC magnetic field of 3.60 T [10]-[11]. The RF interaction structure of the gyrotron oscillator is usually tapered cylindrical cavity made of oxygen-free high conductivity (OFHC) copper material, as shown in Fig.1. The RF fields are mainly concentrated in the middle section of cavity of radius $R_c$. The heat loading of the cavity walls are differential as per cavity RF field profile. Hence, for stable frequency radiation from gyrotron we have to provide an efficient cooling system so that its deformation remains minimum so as to keep the oscillation frequency, RF output power and efficiency deviation remains within the tolerance limit of the device.

### A. Effects of radial deformation on resonant frequency

Gyrotron oscillators operate near to cut-off region of its RF interaction cavity. The cavity radius plays a crucial role in governing the radiation frequency of the RF wave. The cavity radius $R_c$, and the cut-off frequency fc of the interaction cavity of the gyrotron device, are related by [3]:

$$f_c = \frac{\chi_{mp} c}{2\pi R_c}, \qquad (1)$$

where, $c$ is the speed of light and $\chi_{mp}$ is the eigenvalue of the $TE_{mp}$ mode.

Typical 95 GHz gyrotron operating in $TE_{6,2}$ mode, considered provides cavity radius $R_c$ =5.907 mm. Using expression (1), the dependence of cavity cutoff frequency fc with the variations in cavity radius is plotted in Fig. 2. We can observe from this plot that a mild change of cavity radius results in a significant change in the cavity cutoff frequency thereby will cause significant change in the gyrotrons oscillation frequency also. Typically, a 5 μm change in cavity radius results in 80 MHz shift in the device oscillation frequency.

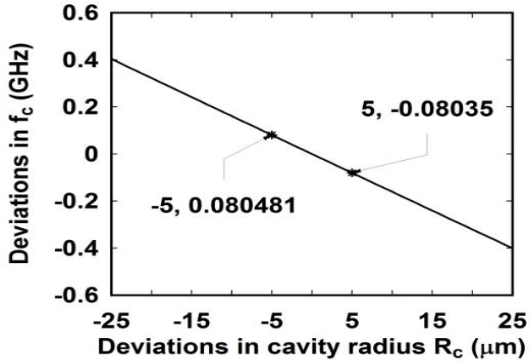


**Fig.2.** Variations in the cavity cut-off frequency $f_c$ due to changes in the RF cavity radius $R_c$.

### B. Wall loss calculation

The Ohmic loss generated in the structure acts as a wall load or heat flux on the structure, and may cause structural deformations. The Ohmic wall losses $P_\Omega$ are connected to the Ohmic quality factor $Q_\Omega$ of the interaction structure by the well-known relation [1]:

$$P_{\Omega} = \frac{2\pi fW}{Q_{\Omega}}, \tag{2}$$

with frequency $f$ and stored energy $W$. A similar expression can be obtained for the diffraction loss $P_{diff}$ as well:

$$P_{diff} = \frac{2\pi fW}{Q_{diff}}. \tag{3}$$

Combining equations (2) and (3), one obtains an expression for the Ohmic loss as a function of the output power $P_{out} = P_{diff}$ as:

$$P_{\Omega} = \frac{P_{diff} Q_{diff}}{Q_{\Omega}}. \tag{4}$$

Under the condition of normal skin effect, one gets:

$$P_{\Omega} \approx \frac{Q_{diff}\left(\pi f \mu_o \sigma\right)}{1-\left(m/\chi_{mp}\right)^2} \frac{P_{diff}}{R_c}, \tag{5}$$

where, σ is the electrical conductivity of the cavity material, m is the azimuthal mode index and μo is the permeability of free space. Dividing equation (5) by the surface area $A$, gives the power loss density of the middle cavity section as [5]:

$$\frac{dP_{loss}}{dA} \approx \sqrt{\frac{1}{30\sigma}}\left(\frac{f^{3/2} P_{out} Q_{diff}}{c^{3/2} L_c}\right)\left(\frac{1}{\chi_{mp}^2 - m^2}\right). \tag{6}$$

The above wall load expression (6) is for a uniform profile and limited to the middle cavity section of length $L_c$ only. Practically, the power loss density in the cavity is of non-uniform nature and also exists at the up-taper section as well. Thus, the ohmic loss profile along the interaction structure can be written as [3]:

$$\frac{dP_{loss}(z)}{dA} \simeq \left(\frac{\delta}{4\pi\mu_0\omega}\right)\left[\frac{1}{\chi_{mp}^2 - m^2}\right] \left(\frac{\chi_{mp}^4}{R^4(z)}\left|V_{mp}\right|^2 + \frac{m^2}{R^2(z)}\left|\frac{dV_{mp}}{dz}\right|^2\right). \tag{7}$$

Here, m is azimuthal mode index, $R(z)$ is the cavity radius at axial position $z$, $V_{mp}$ is the axial electric field profile of the interaction structure resulted from beam wave interaction analysis and δ is the skin depth. The surface roughness effects of interaction cavity can be accounted by replacing $\delta$ with $\delta_{eff} \simeq 2\delta$ [3].

### C. Cooling Fins Design

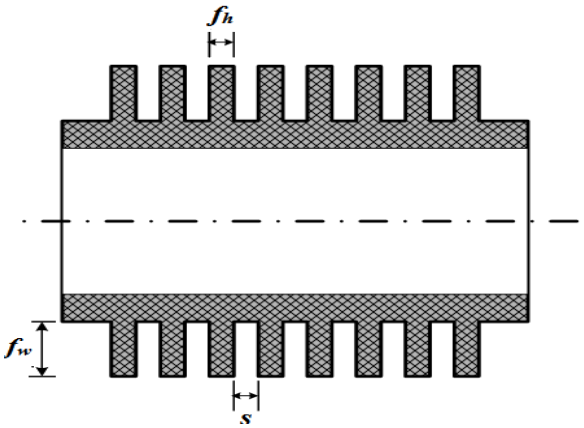


**Fig.3:** Schematic diagram of typical radial cooling fins on a cylindrical surface ($f_h$=fin height, $f_w$=fin width, and $s$= spacing between fins).

For gyrotrons, due to thermal dependency of the materials, efficient heat transfer from the structure is always desired. Generally heat transfer rate can be increased by increasing the temperature gradient between the object and the environment, or by increasing the convection heat transfer coefficient or by increasing the surface area of the object. Here, the concept of increasing the surface area is achieved by incorporating fin surfaces.

Cooling fins provide an extended surface from the object intended to enhance the heat transfer rate to or from the environment through convection by increasing surface area of the object. In the present study, radial fins type as shown in Fig. 3, is considered for the thermal system design.

With radial fins in place, the heat transfer rate qt, is given by [16]:

$$q_t = hA_t\left[1 - \frac{NA_f}{A_t}(1-\eta_f)\right]\theta_b \quad , \tag{8}$$

where, $h$ is the convective heat transfer coefficient, $A_t$ is the total surface area associated with the fins and the object, $N$ is the fins number, each fin surface area $A_f$, single fin efficiency $\eta_f$, and $\theta_b$ is the temperature gradient between outer surface of the object and environment.

Keeping the goal as less fin area for optimum heat transfer rate; by varying fin geometries, such as, width $f_w$, height $f_h$, number of fins $N$ with spacing between fins $s$ is achieved, as shown in Fig. 3.

### D. Heat Transfer Modes in the RF cavity

Heat transfer, defined as the transmission of thermal energy from one region to another as a result of the temperature gradient. It generally takes place by three different modes: Conduction, convection and radiation. The modes of heat transfer are quantified by the appropriate rate equations which give the heat transfer per unit area. In the present problem, heat transfer through the conduction and forced convection modes are chosen to analyze the system.

.

For heat transfer by conduction, the rate equation is known as Fourier's law, and the convective heat transfer process is described by the rate equation known as Newton's law of cooling [16]. The heat transfer from the inner surface to the outer surface of the cavity occurs in the conduction mode and from there on by convection mode to the fluid. The effects of the heat transfer on the cavity due to wall loading can be assessed in terms of surface temperature and radial deformation at the inner and outer walls of the cavity. Heat transfer and structural analyses can be performed using computational fluid domain simulation software, like, ANSYS, STAR-CCM and COMSOL. In the present work, the thermal and structural analysis of the tapered cylindrical RF interaction cavity is carried out adapting a commercial code "COMSOL Multiphysics" whose GUI is more users friendly and simpler to implement than those of ANSYS, used in previously reported work, though is equally accurate [10].

## III. HEAT TRANSFER ANALYSIS USING "COMSOL MULTIPHYSICS"

A commercial code "COMSOL Multiphysics" is adapted here for the thermo-mechanical analysis. This code is a cross-platform finite element analysis solver and multi-physics simulation software. It allows conventional physics-based user interfaces and coupled systems of partial differential equations. In the present study, the heat transfer module and solid mechanics module in COMSOL is chosen for the thermo-mechanical analysis of the interaction structure.

### *A. COMSOL Multiphysics simulation modeling*

Generally investigation process of any problem in COMSOL simulation domain process consists of mainly four steps: 1) modeling of the geometry and assigning materials with given electrical and thermal properties; 2) based on problem investigations, selection of suitable physics modules, assigning the same to the geometry by updating it with the given input conditions, like, type of domain, type of boundaries and initial values, etc.; 3) initializing the study step: by selecting type of study either steady state or time dependent, and coupling between physics modules if necessary; and then 4) Define the mesh distribution by setting sequence type and type of element used for calculations.

**Table I:** RF Interaction cavity parameters

| Parameter | Value (units) |
|---|---|
| Down taper angle, $\theta_d$ | $2.2^0$ |
| Up taper angle, $\theta_u$ | $2.8^0$ |
| Uniform section radius, $R_c$ | 5.907 (mm) |
| Down taper length, $L_d$ | 13 (mm) |
| Middle section length, $L_c$ | 20 (mm) |
| Up taper length, $L_u$ | 26 (mm) |

In the present problem, considering the symmetry nature of the interaction cavity, for geometry realization 2D axis symmetric model in COMSOL is selected and interaction cavity is modeled as per the parameters listed in Table I. From the material library, the OFHC copper with various material properties at 293.5 K as listed in Table II are assigned. The modeled interaction cavity structures without and with radial fins in the COMSOL Multiphysics are shown in the Fig.4.

**Table II:** Cavity material properties at 293.5 K

| Material properties | Value (units) |
|---|---|
| Cavity Material | (OFHC/OF) copper |
| Density | 8939 (kg / $m^3$) |
| Electrical conductivity | $5.8*10^7$ S/m |
| Thermal conductivity | 401 (W / (m. K) ) |
| Specific heat | 383 J / (kg. K) |
| Elasticity modulus | 126 (GPa) |
| Coefficient of Thermal expansion | $1.6719*10^{-5}$ (1/K) |
| Poisson ratio | 0.3351 |

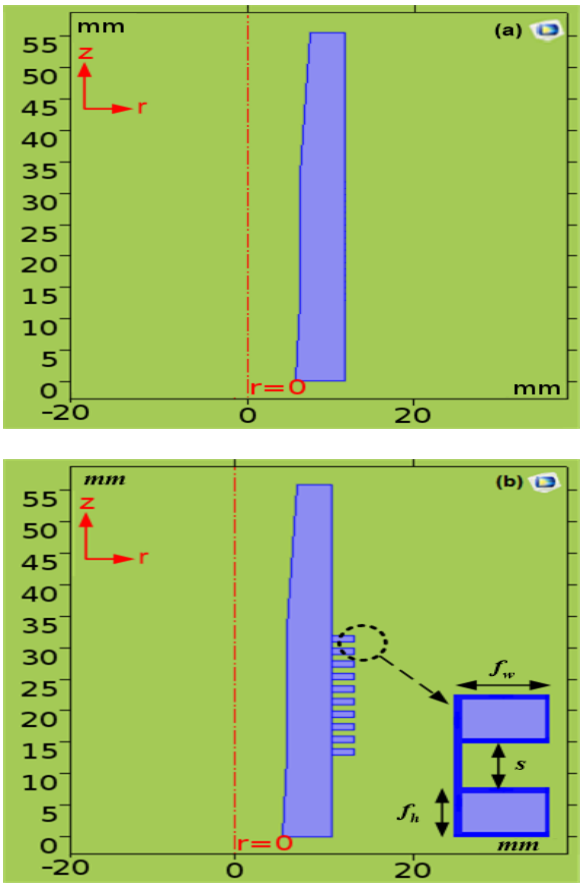


**Fig.4:** 2D axis symmetric interaction cavity models (a) without and (b) with radial fins simulated in COMSOL ($f_h$= fin height, $f_w$=fin width and $s$=spacing between fins).

Heat transfer in solids and solid mechanics physics modules have been selected for the thermal and structural investigations of the interaction structure respectively and both physics are coupled. Coming to the assigning of boundary conditions, in the heat transfer in solids physics module, the wall loading profile (ohmic power loss density) calculated from expression (7) and shown in Fig.5, is loaded as the heat flux at the inner wall surface of the structure which causes the thermal effects and leads to strucural deformations.

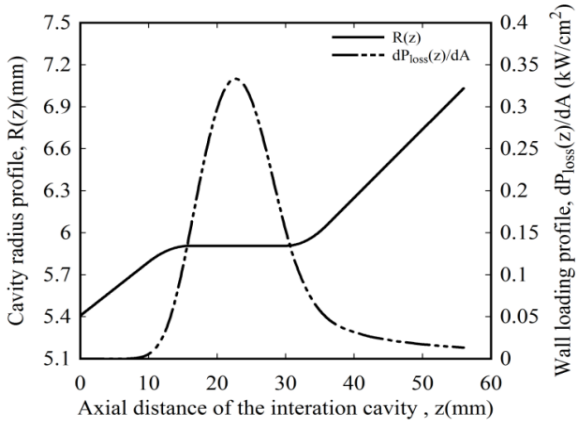


**Fig.5:** Wall loading profile (ohmic power loss density) for operating $TE_{6,2}$ mode of the gyrotron(electrical conductivity σ=5.8x10$^7$ S/m).

Since our goal is to study the thermal effects and thereby designing the optimized cooling system, so the heat flux at the outer cavity walls is chosen in convective heat flux mode that transfers heat from inside to outside surface and thereby restricts the structural deformations, and is explained as:

$$q_o = h(T_{ext} - T_\infty) \quad , \tag{9}$$

where $T_{ext}$ is the outer surface temperature of the structure and $T_\infty$ is the ambient temperature. Since, the heat transfer takes from high temperature to low temperature so in the present problem it occurs from inner surface to outer surface that allows surface deformation from inner to outer surface [16]. In the present study, by fixing ambient temperature $T_\infty$ at 293.5 K, for various convective heat transfer coefficient $h$ (W/m$^2$.K) values the simulations are carried out. The axial end surfaces of the interaction cavity not subjected to heat flux are thermally insulated for the study.

The temperature distribution of the interaction cavity resulted from the heat transfer in solids physics module is coupled to the solid mechanics physics module as thermal load for the deformations study. Maintained fixed constraints on the axial end surfaces and free to move constraints on the radial surfaces of the interaction cavity, the structural deformations have been calculated. A steady-state, with coupling between physics modules study and sequence type of physics controlled mesh with extremely fine element type is selected for the simulations.

Firstly, the thermo-mechanical analysis using COMSOL Multiphysics code is performed by considering various thickness values of the interaction cavity from the middle section, $\delta R$= 3 mm to 7 mm at different values of heat transfer coefficient $h$ of the coolant under no fins condition. Then, by considering radial fins over the middle section with various fin width $f_w$, fin height $f_h$, spacing between fins $s$, and different number of fins $N$, the thermo-mechanical analyses on interaction cavity are also carried out.

In the present work, considering radial fins along the middle section of the cavity ($L_c$), the thermal system is optimized by maintain the temperature of coolant at room temperature. The allowed tolerances of radial deformations (increase) at the inner cavity radius is upto 6 μm such that oscillation frequency shifts at maximum upto 0.1 GHz [3] with average outer surface cavity temperature ~ 300 K. For this purpose, different convective heat transfer coefficient $h$ values are chosen which solely describe the fluid dynamics parameters [17], such as, fluid flow rates, hydraulic diameter, etc. Generally, in forced convection mode, for liquids, heat transfer coefficient $h$ lies in the range between 100-20000 (W/m$^2$.K) and for convection with phase change boiling or condensation; the heat transfer coefficient $h$ lies in the range of 2500-100000 (W/m$^2$.K) [17]. In the present problem, the study is limited with heat transfer coefficient $h$ from 4000 to 20000 (W/m$^2$.K), means no boiling or condensation of the fluid in the cooling system design is allowed. The impact of thermal system parameters on the RF interaction cavity under the ohmic wall loss are assessed in terms of cavity outer surface temperatures by thermal analysis and radial deformations at cavity inner surfaces by structural analysis and are discussed in details in Section IV. Subsequently, the thermo-mechanical effects on the RF behavior of the interaction cavity at optimized cooling system parameters are investigated using the nonlinear time-dependent multimode theory [3], [11]-[15].

## IV. RESULTS AND DISCUSSION

The thermo-mechanical effect of ohmic loss generated due to the microwave power radiated in the tapered cylindrical interaction cavity of the gyrotron has got investigated. The structure is modeled and simulated using commercial code "COMSOL Multiphysics". In this paper, considering various cavity thickness $\delta R$ values at different convective heat transfer coefficient $h$ values, for without fins and with radial fins groups are studied. Initially, investigations are carried out for structure without fins, labeled as "WOG" group. As described in Section III, the effects are measured in terms of radial deformations (increase) $\Delta R_{rad}$ at inner and temperatures $T_{out}$ at outer surface of the interaction cavity. Since, due to the non-uniform nature of the heat flux, for the initial study, both the average and maximum values of inner $\Delta R_{rad}$ and $T_{out}$ at inner and outer surfaces are plotted as Figs. 6 - 9, respectively.

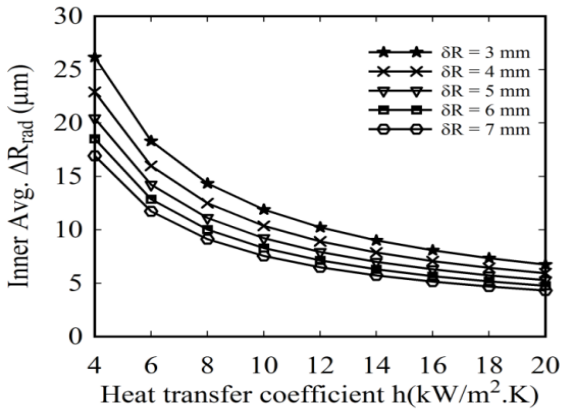


**Fig.6:** Average radial deformation$\Delta R_{rad}$ at the cavity inner surface for various heat transfer coefficient $h$ and cavity thickness $\delta R$ values.

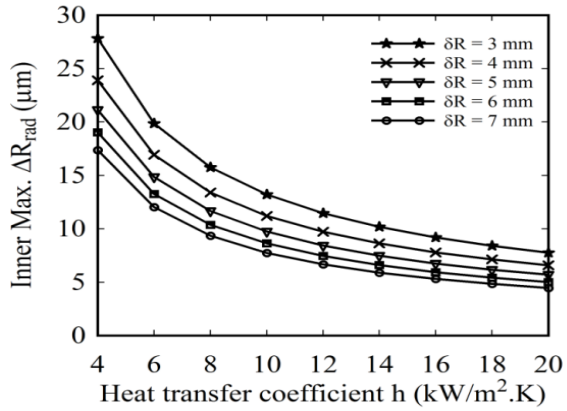


**Fig.7:** Maximum radial deformations $\Delta R_{rad}$ at the cavity inner surface for various heat transfer coefficient $h$ and cavity thickness $\delta R$ values.

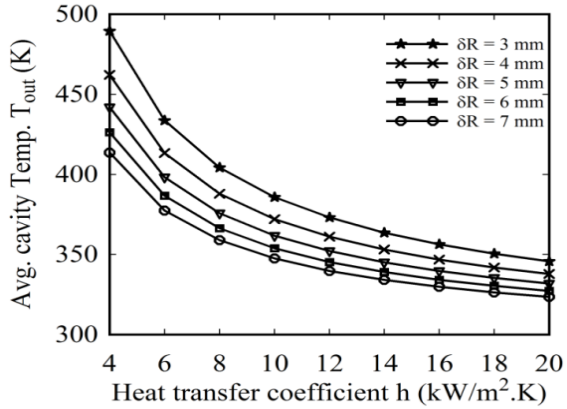


**Fig.8:** Average temperature at the cavity outer surface $T_{out}$ for various heat transfer coefficient $h$ and cavity thickness $\delta R$ values.

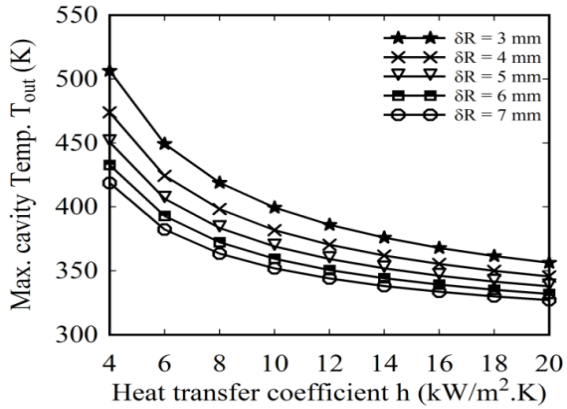


**Fig.9:** Maximum temperature at the cavity outer surface $T_{out}$ for various heat transfer coefficient $h$ and cavity thickness $\delta R$ values.

As expected, it can be easily observed from the Figs. 6-9 that for higher values of convective heat transfer coefficient $h$, the amount of radial deformations (increase) and the temperature values of the cavity are decreasing monotonically with increasing of cavity thickness $\delta R$ means increment in the heat transfer rate. In order to restrict the magnitudes of radial deformations (increase) $\Delta R_{rad}$ and the cavity temperatures $T_{out}$ under the desired values, radial type fins have been introduced on the outer surface of the interaction cavity. From the preliminary studies without fins (WOG group), the probable range of convective heat transfer coefficient $h$ and cavity thickness $\delta R$ are suitable for the optimum thermal system design of cavity structure are selected. Secondly, there is a nominal variation in the average and maximum levels of radial deformations $\Delta R_{rad}$ at the inner surface, as well as considering the temperatures at the outer surface the average surface $T_{out}$ are of important for the optimization of the thermal design. Thus, the variations of maximum inner radial deformations (increase) $\Delta R_{rad}$ and average outer surface temperatures $T_{out}$ for the fin groups are shown in the rest of the analysis.

As mentioned in Section II, achieving the desired performance of the thermal system with minimum fins area is always desired. As discussed in Section III, the fins area is increased by varying the fins geometrical parameters in a systematic way and simultaneously observing the maximum radial deformations (increase) and average temperature values of the interaction cavity by using COMSOL Multiphysics. Considering moderate power levels in the interaction cavity, the radial fin groups labeled as RG1, RG2, RG3, and RG4 are placed in the middle part region ($L_c$) on the outer surface of the RF interaction cavity. Different geometrical parameters of the fin groups are listed in Table III with uniform spacing $s$=1 mm between the fins.

**Table III:** Dimension of various radial fin groups

| Fin group | Fin width $f_w$ (mm) | Fin height $f_h$ (mm) | Number of fins N |
|---|---|---|---|
| WOG | 0 | 0 | 0 |
| RG1 | 2 | 1 | 10 |
| RG2 | 2.5 | 1 | 10 |
| RG3 | 3 | 1 | 10 |
| RG4 | 3.5 | 1 | 10 |

The thermo-mechanical simulations are carried out with the various fins groups for the range of convective heat transfer coefficient $h$ from 8000 to 16000 (W/m$^2$.K), and cavity thickness $\delta R$=3 mm to 5 mm. Maximum inner radial deformation (increase) $\Delta R_{rad}$ and average cavity outer surface temperatures $T_{out}$ for the fin groups are tabulated in Table IV and Table V.

**Table IV:** Maximum values of radial deformations (increase) $\Delta R_{rad}$ at cavity inner surface for various radial fin groups (RG1, RG2, RG3, RG4) at various heat transfer coefficient h and thickness δR values.

| Heat transfer coefficient $h$ (W/m$^2$.K) | $\delta R$, mm | WOG $\Delta R_{rad}$ (μm) | RG1 $\Delta R_{rad}$ (μm) | RG2 $\Delta R_{rad}$ (μm) | RG3 $\Delta R_{rad}$ (μm) | RG4 $\Delta R_{rad}$ (μm) |
|---|---|---|---|---|---|---|
| 8000 | 3 | 15.752 | 6.920 | 6.070 | 5.424 | 4.907 |
| 8000 | 4 | 13.384 | 6.186 | 5.084 | 4.554 | 4.135 |
| 8000 | 5 | 11.672 | 5.608 | 4.416 | 3.967 | 3.614 |
| 10000 | 3 | 13.211 | 5.774 | 5.474 | 4.921 | 4.483 |
| 10000 | 4 | 11.205 | 5.164 | 4.584 | 4.137 | 3.782 |
| 10000 | 5 | 9.742 | 4.682 | 3.986 | 3.609 | 3.311 |
| 12000 | 3 | 11.465 | 5.000 | 5.011 | 4.582 | 4.297 |
| 12000 | 4 | 9.717 | 4.476 | 4.200 | 3.853 | 3.625 |
| 12000 | 5 | 8.433 | 4.061 | 3.657 | 3.365 | 3.174 |
| 14000 | 3 | 10.182 | 4.441 | 4.807 | 4.405 | 4.151 |

| | | | | | | |
|---|---|---|---|---|---|---|
| 14000 | 4 | 8.629 | 3.980 | 4.010 | 3.716 | 3.521 |
| 14000 | 5 | 7.479 | 3.614 | 3.484 | 3.254 | 3.097 |
| 16000 | 3 | 9.193 | 4.016 | 4.653 | 4.248 | 4.016 |
| 16000 | 4 | 7.794 | 3.605 | 3.900 | 3.599 | 3.421 |
| 16000 | 5 | 6.751 | 3.277 | 3.402 | 3.163 | 3.020 |

**Table V:** Average cavity outer surface temperatures of various radial fin groups (RG1, RG2, RG3, RG4) at various convective heat transfer coefficient *h* and cavity thickness *δR* values.

| Heat transfer coefficient *h* (W/m2.K) | *δR* mm | WOG $T_{out}$ (K) | RG1 $T_{out}$ (K) | RG2 $T_{out}$ (K) | RG3 $T_{out}$ (K) | RG4 $T_{out}$ (K) |
|---|---|---|---|---|---|---|
| 8000 | 3 | 404.2 | 339.9 | 333.3 | 328.1 | 323.9 |
| 8000 | 4 | 387.8 | 334.4 | 328.8 | 324.3 | 320.6 |
| 8000 | 5 | 375.7 | 330.1 | 325.1 | 321.2 | 318.0 |
| 10000 | 3 | 385.8 | 331.0 | 325.5 | 321.2 | 317.8 |
| 10000 | 4 | 372.0 | 326.5 | 321.8 | 318.1 | 315.2 |
| 10000 | 5 | 361.7 | 323.0 | 318.9 | 315.6 | 313.0 |
| 12000 | 3 | 373.0 | 325.0 | 320.3 | 316.7 | 313.8 |
| 12000 | 4 | 361.1 | 321.2 | 317.2 | 314.0 | 311.5 |
| 12000 | 5 | 352.2 | 318.2 | 314.7 | 311.9 | 309.7 |
| 14000 | 3 | 363.6 | 320.6 | 316.5 | 313.4 | 310.8 |
| 14000 | 4 | 353.0 | 317.3 | 313.8 | 311.1 | 308.9 |
| 14000 | 5 | 345.1 | 314.7 | 311.7 | 309.3 | 307.3 |
| 16000 | 3 | 356.3 | 317.3 | 313.7 | 310.9 | 308.7 |
| 16000 | 4 | 346.8 | 314.4 | 311.3 | 308.9 | 307.0 |
| 16000 | 5 | 339.7 | 312.1 | 309.4 | 307.3 | 305.6 |

For the radial fin groups RG3 and RG4, the range of h from 14000 to 16000 with δR = 5 mm, the maximum inner radial increase is less than 3.25 µm which is of our design constraint and the average cavity outer surface temperature is at 310 K.

For the optimum range of heat transfer coefficient *h* values, considering water as a coolant with $T_{fluid}$ at 293.15 *K*, the range of various thermal system parameters, like, hydraulic diameters ($D_h$) through which the coolant is flown, at different water flow rates are calculated and are shown in the Fig. 10 [16].

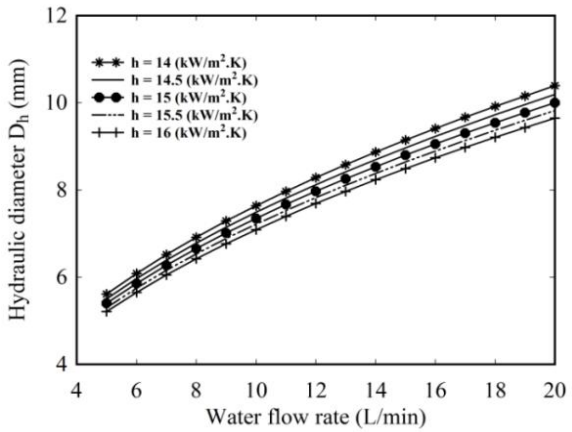


**Fig.10:** Range of hydraulic diameter $D_h$ and Water flow rates of the thermal system for the optimized convective heat transfer coefficient *h* values.

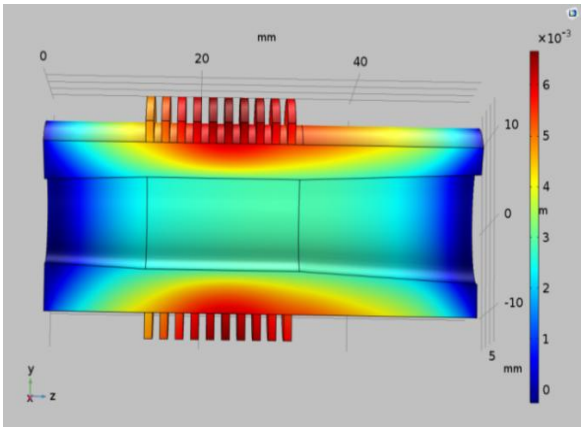


**Fig.11:** 3D view of the radial deformation distribution for heat transfer coefficient *h*=15000 (W/m2.K) and *δR*=5 mm of RG3 group.

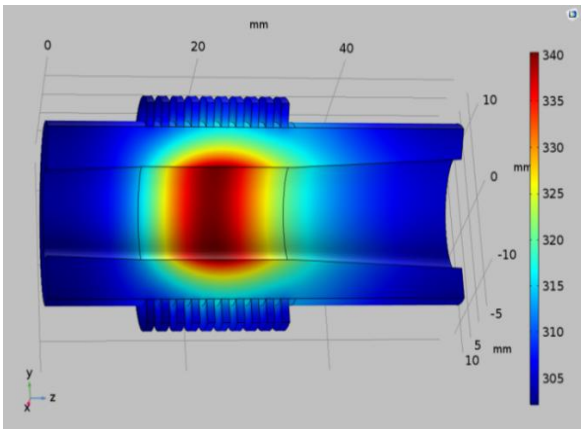


**Fig.12:** 3D view of temperature distribution for heat transfer coefficient *h*=15000 (W/m$^2$.K) and cavity *δR*= 5 mm of RG3 group.

The 3D view of temperature distribution and the radial deformation (increase) distribution of interaction cavity for optimized heat transfer coefficient *h* as 15000 (W/m$^2$.K) and cavity thickness *δR*=5 mm, for RG3 fins group, are shown in Figs.11 and 12.

It can be observed that the average value of cavity outer surface temperature $T_{out}$ is around 308*K* and the maximum radial increase $\Delta R_{rad}$ at the inner surface of the cavity is ~3.2µm that is within tolerable limits of the targeted design parameters. The deformations occurring around the outer surface is of maximum 6 µm, a collective one from inner to outer surface. Comparatively, the surface deformation at the inner walls is more because of the presence of heat source which causes larger temperature rise than the coolant temperature. Due to the coolant, the heat transfers faster to the outer surface thereby maintaining desired operation. The cavity radius profiles of initial and the deformed cavity with in tolerable limits at the optimized cooling system parameters are shown in Fig. 13.

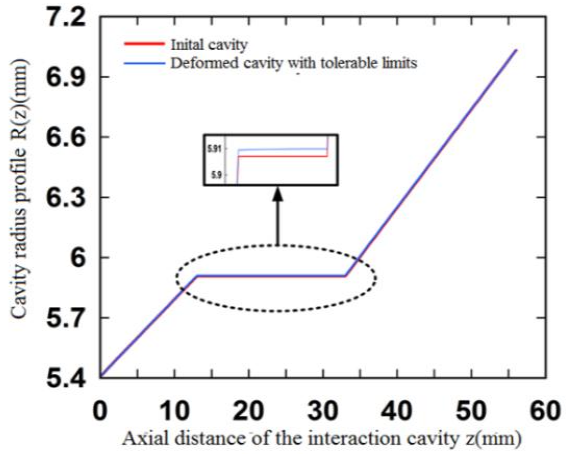


**Fig.13:** Initial (red color) and deformed cavity (blue color) due to ohmic loss at optimized thermal system parameters.

Now, the study is further extended to investigate thermo-mechanical effects on the RF behavior of the deformed cavity with tolerable limits at initial and final (steady state) conditions. RF behavior of the device under both conditions, cold (in absence of electron beam) as well as hot (in presence of electron beam) are investigated. At cold condition, the axial RF field profile and the resonant frequency and quality factors of the cavity are calculated by solving the wave equation in the cavity at radiation boundary conditions that leads minimum reflection [3]. The comparisons of cavity field amplitudes with resonance frequency and quality factors of both initial and deformed conditions (with RG3 fins, $h$ =15000 W/m$^2$.K, $\delta R$ = 5 mm) are plotted in Fig.14. It can be observed that with designed cooling system, maximum reduction in the resonant frequency $f_{res}$ is 48 MHz and a decrement of 20 in the diffractive quality factor $Q_{diff}$ occurred from the initial cavity values (cold condition).

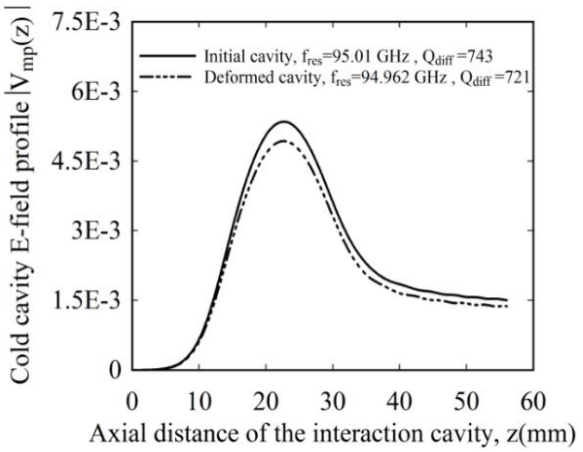


**Fig.14:** Cold cavity field amplitude profiles for the initial and deformed cavity.

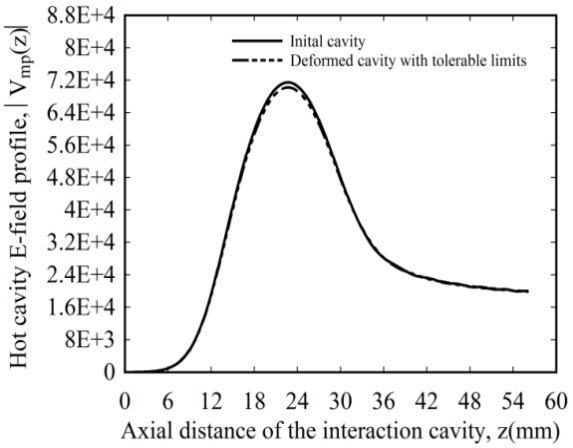


**Fig.15:** Hot cavity electric field profiles of initial and deformed cavity.

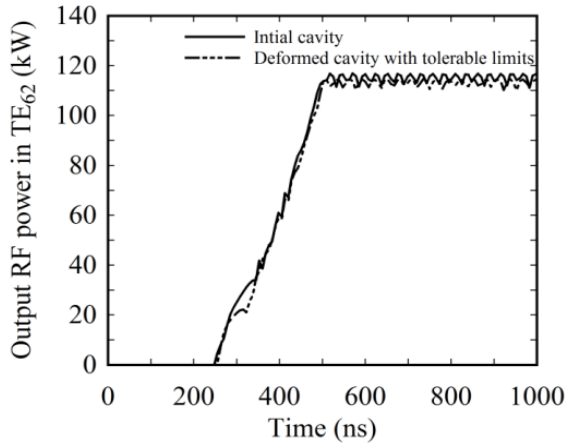


**Fig.16:** Comparisons of power levels in the $TE_{6,2}$ for initial and deformed cavity.

To study the effect of cavity deformation under hot (in presence of electron beam) condition, we have used non-linear, time dependent, multimode theory of the gyrotrons [3],[11]-[13]. Maintaining the same beam parameters with zero velocity spread, gyrotron device performance with the deformed RF interaction cavity is obtained. The field amplitude profile and power levels in various modes are calculated. Comparisons of hot cavity field amplitude profiles and the output power levels in the operating modes $TE_{6,2}$ for initial and deformed cavity with tolerable limits are plotted in Figs.15 and 16. It can easily be noted a reduction of 2 kW in RF output power in the case for the deformed cavity from the initial cavity gyrotron device.

## V. CONCLUSION

Thermal and structural analysis of a tapered cylindrical RF interaction cavity of a $TE_{6,2}$, 95 GHz, 100 kW gyrotron is carried out to study the effect of ohmic loss generated due to radiated microwave energy. For stable device operation, with the help of design relationships, radial cooling fins design for the cavity is presented.

Describing the approach, an optimum thermal system is designed and performance is simulated using a commercial code "COMSOL Multiphysics". Implementation of this code is simpler than those previously reported though equally accurate. Thermo-mechanical behavior of the interaction cavity structure for various cavity thicknesses, and convective heat transfer coefficient values under without fins and with radial fins conditions are investigated. Considering water as coolant at room temperature ~293 K, the range of hydraulic diameter and flow rates are determined for the optimum convective heat transfer coefficient values from 14000 - 16000 W/m$^2$.K. An optimized simple cooling system thus designed keeps the maximum RF cavity radius deformation (increase) ~ 3.2 µm maintaining the average cavity outer surface temperature of 308 K. Further, nonlinear time-dependent multimode analysis is carried out to observe the RF output behavior of the gyrotron. A decrease in its resonance frequency of 48 MHz and a decrement of 20 in the diffractive quality factor of the RF interaction cavity with the reduction of 2 kW of RF output power are observed in the case for the deformed cavity from those of the initial cavity gyrotron device, which are within the tolerance limit of such devices. We hope that the thermo-mechanical analysis, radial cooling fins and cooling system design, its optimization as well as description of simpler simulation technique using commercial code "COMSOL Multiphysics" for the gyrotron RF interaction cavity presented in this work will be useful not only to the tube designers but also to the high power microwave system developers.

## REFERNECES


1. C. Edgecombe, *Gyrotron Oscillators*. Florida: CRC Press, 1993.
2. MK Thumm, State-of-the-Art of High Power Gyro-Devices and Free Electron Masers. Update 2017 (KIT Scientific Reports; 7750). KIT Scientific Publishing, Vol. 7750, 2018.
3. M. V. Kartikeyan, E. Borie, and M. Thumm, *Gyrotrons: High-Power Microwave and Millimeter Wave Technology*. Germany: Springer Science & Business Media, 2013.
4. V. Flyagin, A. Gaponov, I. Petelin, and V. Yulpatov, "The gyrotron," *IEEE Transactions on Microwave Theory and Techniques*, Vol. 25 ( 6), 1977, pp. 514–521.
5. G. S. Nusinovich, M. K. Thumm, and M. I. Petelin, "The gyrotron at 50: Historical overview," *Journal of Infrared, Millimeter, and Terahertz Waves*, Vol. 35(4), 2014, pp. 325–381.
6. A. Kumar, N. Kumar, U. Singh, H. Khatun, V. Vyas and A. K. Sinha, "Thermal and structural analysis and its effect on beam-wave interaction for 170-GHz, 1-MW gyrotron cavity" *Journal of fusion energy*, Vol. 31(2), 2012, pp. 164–169.
7. Q. Liu, Y. Liu, X. Niu, Z. Chen, H. Li, J. Xu, and J. Zhao, "Thermoanalysis and Its Effect on the Multimode Beam-Wave Interaction for a 0.24-THz, Megawatt-Class Gyrotron," *IEEE Transactions on Electron Devices*, Vol. 65(2),2018, pp. 704–709.
8. Q. Liu, Y. Liu, Z. Chen, X. Niu, H. Li, and J. Xu, "Investigation on heat transfer analysis and its effect on a multi-mode, beam-wave interaction for a 140 GHz, MW-class gyrotron," *Physics of Plasmas*, Vol. 25(4),2018, p. 043101.
9. J. Koner and A. K. Sinha, "Wall loss and thermal analysis of 200 kW (CW), 42 GHz Gyrotron cavity" International Journal of Microwave Optical Technology, Vol. 4, no. 1, pp. 18–20, (2009).
10. D. Salvi, DorinBoldor, J. Ortego, G. M. Aitaand C. M. Sabliov Numerical Modeling of Continuous Flow Microwave Heating: A Critical comparison of COMSOL and ANSYS, *Journal of Microwave Power and electromagnetic Energy*, vol. 44(4),2010 ,pp.187-197.
11. B. Danly and R. J. Temkin, "Generalized nonlinear harmonic gyrotron theory," *The Physics of fluids*, Vol. 29 (2), 1986, pp. 561–567.
12. A. Fliflet, R. Lee, S. Gold, W. Manheimer, and E. Ott, "Time-dependent multimode simulation of gyrotron oscillators," *Physical Review A*, Vol. 43(11), 1991, p. 6166.
13. A. Singh, B. Ravi Chandra, and P. K. Jain, "Multimode behavior of a 42 GHz, 200 KW gyrotron," *Progress In Electromagnetics Research*, Vol. 42, 2012, pp. 75–91.
14. VGB8095Gyrotronoscillator https://www.cpii.com/docs/datasheets/0/vgb8095.pdf.
15. S. V. Rao, and P. K. Jain, "PIC Simulation of a W-band Gyrotron Oscillator," in *National Workshop on Vacuum Electron Devices & its Applications. VEDA*, Bangalore, India, 2015.
16. J. M. Gere, S. P. Timoshenko, *Mechanics of Materials*. India: CBS Publishers& Distributors PVT. LTD, 2004.
17. F. P. Incropera, A. S. Lavine, T. L. Bergman, and D. P. DeWitt, *Principles of Heat and Mass Transfer*. USA: Wiley, 2013.


## AUTHORS PROFILE

**Sivavenkateswara Rao V** received the B.Tech. degree in electronics and communication engineering from JNTU, Hyderabad, India, in 2008, and the M.Tech. degree in digital systems from MNNIT Allahabad, , India, in 2012. He is currently pursuing the Ph.D. degree in microwave vacuum electron beam devices from IIT (BHU) varanasi. His current research interests include beam wave interaction and thermal studies of high power gyrotrons.

**Muthiah Thottappan** (M'14) received the Ph.D. degree in microwave engineering from IIT Varanasi, Varanasi, India, in 2013. He is currently an Assistant Professor with the Department of Electronics Engineering, IIT (BHU) Varanasi. His current research interests include RF & Microwave Engineering, High Power Microwave (HPM) Devices.

**Pradip Kumar Jain** (SM'05) received the B.Tech. degree in electronics engineering and the M.Tech. and Ph.D. degrees in microwave engineering from IIT (BHU) Varanasi, Varanasi, India, in 1979, 1981, and 1988, respectively. He is currently a Professor with the Department of Electronics Engineering, IIT Varanasi. His current research interests include High Power RF / Microwave Devices, Circuits and Systems. RF MEMs, Metamaterial devices Microwave Imaging and Remote Sensing.